Japanese Journal of Gastroenterology and Hepatology

Research Article

ISSN: 2435-1210 | Volume 9

BCHE As A Prognostic Biomarker For Stomach Adenocarcinoma And Correlates With Immune Cells Infiltration

Jikai He[1#], Xiaobing Yang[2#], Bin Wang[2], Lizhou Jia[1], Wei Zhao[2,1*] ,Yanqiang Huang[1,3*]

[1]Research Center for the prevention and treatment of drug resistant microbial infecting, Youjiang Medical University for Nationalities, 533000 Baise, China

[2]Department of Pathology, Nanjing First Hospital, Nanjing Medical University, 210006 Nanjing, China

[3]Guangxi University Key Laboratory of Basic and Translational Oncology and Infectious Diseases, Youjiang Medical University for Nationalities, 533000 Baise, China

[#]Jikai He and Xiaobing Yang are co-first authors of the article

[*]Corresponding author:

Yanqiang Huang and Wei Zhao,
Research Center for the prevention and treatment of drug resistant microbial infecting, Youjiang Medical University, Department of Pathology, Nanjing First Hospital, Nanjing Medical University, Guangxi University Key Laboratory of Basic and Translational Oncology and Infectious Diseases, Youjiang Medical University for Nationalities, China,
E-mail : 00435@ymcn.edu.cn; zhaowei_njmu@163.com

Received: 10 Oct 2022
Accepted: 20 Oct 2022
Published: 25 Oct 2022
J Short Name: JJGH

Citation:

Yanqiang Huang and Wei Zhao. SBCHE As A Prognostic Biomarker For Stomach Adenocarcinoma And Correlates With Immune Cells Infiltration.. J Gstro Hepato. V9(10): 1-17

Keywords:

BCHE, Stomach Adenocarcinoma, Prognosis, Tumor-infiltrating Immune Cells, Mutation

Abbreviations:

(I) Conception and design: Wei zhao and Yanqiang Huang. (II) Administrative support: Wei zhao. (III) Collection and assembly of data: Jikai He and Xiaobing Yang (IV) Data analysis and interpretation: Jikai He, Lizhou Jia and Bin Wang. (V) Manuscript writing: All authors. (VI) Final approval of manuscript: All authors.

1. Abstract

1.1. Background: Bcylcholinesterase (BCHE) is a nonspecific esterase synthesized by the liver that promotes cell proliferation and differentiation. Several studies suggested that BCHE is related to the occurrence and development of some tumors. However, the expression of BCHE in stomach adenocarcinoma (STAD) and its regulatory mechanism remains elusive.

1.2. Research Design and Methods: Genomic data and clinical data of STAD were obtained from UCSC Xena. The prognostic gene BCHE was screened by Lasso-penalized Cox regression analysis; And the correlation between the expression level of BCHE mRNA and clinicopathological information were examined. Moreover, the relationships between BCHE mRNA and immune landscape, functional enrichment, mutation, DNA methylation and drug sensitivity were explored.

1.3. Results: 15 genes related to the prognosis of STAD patients were screened out through Lasso regression analysis, and the BCHE gene with the most obvious differential expression ($P < 0.001$). Further analysis indicated that high expression of BCHE mRNA in advanced stage STAD, and predicted poorer OS; meanwhile the expression of BCHE in tumor cells is closely related to immune cell infiltration and immune reactivity related molecules; and BCHE mRNA was mainly expressed in fibroblasts through single-cell sequencing analysis. Enrichment analysis showed that the high expression of BCHE mRNA was related to cell proliferation, differentiation and other related signaling pathways. The study also found that the total mutation rate of BCHE in STAD patients was 10.17%, in which amplified mutations accounted for 50%. And the BCHE mutation had a worse prognosis, but BCHE hypermethylation had a better prognosis in STAD patients. Finally, BCHE mRNA expression was

negatively correlated with TMB in STAD patients, and positive associated with several types of drug sensitivity.

1.4. Conclusions: BCHE as a prognostic biomarker for STAD and the regulatory mechanism of BCHE might be related with its function in cell proliferation, differentiation and other related signaling pathways.

2. Introduction

Gastric cancer (GC) is the fifth most common cancer in the world, with the fourth highest death rate [1,2]. In 2020, around 1,089,103 people were newly diagnosed and 768,793 people died worldwide[3]; moreover, GC is relatively common in China [4], and about 95% are stomach adenocarcinoma (STAD). The current treatment methods for STAD mainly include surgery, radiotherapy and chemotherapy, but the incidence of postoperative local recurrence or distant metastasis exceeds 40% [5]. Besides, there are obvious side effects after radiotherapy and chemotherapy, which leads to the 5-year survival rate of STAD patients only about 20%-40% [6,7]. Therefore, it has become an urgent public health issue to explore the potential mechanism of the occurrence and progression of STAD and to find new therapeutic and prognostic targets that can improve the survival rate of STAD patients.

To screen out the genes related to prognosis of STAD, the study performed multiple analysis methods, and found that BCHE has good prognostic value for STAD. Butyrylcholinesterase (BCHE) is a plasma enzyme, produced in the liver and secreted into the blood, which catalyzes the hydrolysis of butyrylcholine, succinylcholine, and many other esters [8].BCHE is mainly expressed in exosomes and endoplasmic reticulum, located in 3q26.1-q26.28 [9]. BCHE has a half-life of about 12 days and a normal value between 5900 and 13200 IU/L [10, 11]. Increased activity of this enzyme has been reported in patients with diseases such as obesity, diabetes, uremia, hyperthyroidism and hyperlipidemia [12-14]; meanwhile, serum levels of BCHE have been significantly reduced in a variety of cancers, including prostatic cancer [15], oral cancer [16], pancreatic cancer [17] and cervical cancers [18]. However, the expression level and regulation mechanism of BCHE gene in STAD, as well as its correlation with clinical treatment and prognosis are still unclear.

In this study, the dataset of STAD patients were obtained from the UCSC Xena database. The prognostic gene BCHE was screened by Lasso-Penalized Cox regression analysis, and the correlation between BCHE mRNA expression level and clinicopathological information and prognosis of STAD were analyzed. Next, we studied the correlation between BCHE mRNA in STAD and immune infiltrating cells and immune reaction-related molecules through multiple databases and algorithms. We also analyzed the pathway mechanism of BCHE in STAD by enrichment analysis. Finally, we used the cBioPortal database to analyze the mutation form of BCHE in STAD and its correlation with prognosis. The results of this study demonstrated that BCHE is a predictable biomarker in STAD and can help predict the prognosis of STAD patients.

3. Materials and Methods

3.1. Data download and processing

The gene expression data and clinical data of STAD patients were obtained from the TCGA database, which the data were downloaded from the UCSC Xena database (https://xenabrowser.net/datapages/) [19]. Xena's STAD gene expression data, we selected 409 samples with complete pathological information for further analysis. In addition, the BCHE DNA methylation and mutation data were obtained from the cBioPortal database, and the spatial transcriptomics data were obtained from the 10× database.

3.2 Prognostic risk assessment model construction for STAD

By using the "tidyverse" package in R software (version 4.1.2), set log FC>2, P value <0.05, and a total of 1640 genes were screened. We performed Lasso-penalized Cox regression analysis on these genes [20]. We used Cox proportional hazards regression analysis to assess the power of overall survival (OS) in patients with STAD. 15 genes were filtered based on the best lambda value. According to the regression coefficient and expression level of each gene, the risk score was calculated to establish an risk score model. The risk score was determined using the following formula for every patient: Risk score = (0.00464 * expressionGPX3) + (0.00128 * expressionBCHE) + (-0.00292 * expressionSOX14) + (0.03080 * expressionADAMTS18) + (0.00189 * expressionASPA) + (0.01107 * expressionCD36) + (0.06397 * expressionSERPINE1) + (0.01348 * expressionCYP19A1) + (0.00802 * expressionLRAT) + (0.05716 * expressionCGB5) + (0.000098 * expressionANO3) + (0.01877 * expressionCYMP) + (0.04104 * expressionCFHR4) + (0.00942 * expressionF13B) + (0.01341 * expressionOTX2).

3.3 Chi-square test, forest plot and nomogram analysis

We performed a chi-square test on the clinicopathological information by SPSS18.0 software. We used the "forestplot" package to plot the forest plot [21]. Nomograms were constructed based on independent prognostic factors (clinicopathological information, risk score and BCHE expression level) by "rms" R package of R software [22].

3.4 Immune Infiltration Analysis

We used the ESTIMATE algorithms to evaluate each TCGA sample by scoring immune cells, tumor purity, and stromal cells, and divided TCGA samples into high and low groups via the 50% cut-off [23] for further analysis. The CIBERSORT algorithm was used to estimate the proportion of different immune cells in cancer tissue (the infiltration level of 22 immune cells in STAD), and the differences of immune cells between high and low BCHE groups in STAD tissue were explored [24]. We performed single-sample gene set enrichment analysis (ssGSEA) by the R package GSVA [25]. We calculated the degree of infiltration of 28 immune cell types based on gene expression levels

3.5 TIMER2.0 database

TIMER2.0 (Tumor Immune Estimation Resource) database *(https://cistrome.shinyapps.io/timer/)* [26] uses RNA-seq expression profiling data to detect immune cell infiltration in tumor tissue. 10,897 samples from The Cancer Genome Atlas (TCGA) of 32 cancer types were used to estimate the abundance of immune infiltrates.

3.6 TISIDB

TISIDB: an integrated repository portal for tumor-immune system interactions (http://cis.hku.hk/TISIDB/index.php) [27]. Determine the correlation between BCHE expression and molecules associated with lymphocytes and immune responses in cancer..

3.7 String database

STRING: functional protein association networks (https://string-db.org/) online platform [28]. We select the 20 proteins most closely related to BCHE protein, construct a protein-protein interaction network.

3.8 The Human Protein Altas Database

The protein expressions of BCHE in human normal tissues and tumor tissues were validated via the Human Protein Altas, The single-cell sequencing results of BCHE were validated via the Human Protein Altas (HPA, *https://www.proteinatlas.org/)* [29].

3.9 Ten-x (10x) genomics database

The colorectal cancer spatial transcriptomic data of the BCHE were derived from the 10x genomicsdatabase *(https://support.10xgenomics.c)[](30). om)* [30].

3.10 Cancer Cell Line Encyclopedia database

The expression level of BCHE mRNA in gastric cancer cell lines was studied through Cancer Cell Line Encyclopedia database. (CCLE, *https://sites.broadinstitute.org/ccle/)* [31].

3.11 Gene set and functional enrichment analysis

The DAVID Bioinformatics Resources database (https://david.ncifcrf.gov/)(32) was used for Gene Ontology (GO) functional analysis of BCHE genes to understand the biological process of the target, the Kyoto Encyclopedia of Genes and Genomes (KEGG) pathway was used to analyze the main signaling pathways(33). The gene set enrichment analysis (GSEA) analysis were performed through the R package "ClusterProfiler"(25).

3.12 SangerBox3.0 database for data visualization

SangerBox3.0 database (http://vip.sangerbox.com/), with powerful data visualization function, brings together dozens of databases around the world, updated synchronously every day, with 150,000 human genes, 30 million research articles, 10,000 biomedical journals, nearly 20 years of fund data, and 300,000 sample datasets [34].

3.13 CBioPortal database

CBioPortal for Cancer Genomics (http://www.cbioportal.org) is an integrated database of genetic data types including somatic mutations, DNA methylation , protein abundance, mRNA and microRNA expression and DNA copy number alterations,. We provide visualization and multidimensional cancer genomics data [35]. Based on TCGA database, we obtained histograms of mutation statistics and associated KM survival curves of the BCHE gene from cBioPortal.

3.14 Tumor Mutation Burden (TMB)

The correlation between BCHE gene expression and TMB was analyzed by the SangerBox3.0 database (http://vip.sangerbox.com/) [34].

3.15 RNAactDrug database

RNAactDrug is a comprehensive resource for querying associations between drug sensitivity and RNA molecules, which including mRNAs, lncRNAs and miRNAs at four molecular levels (expression, copy number variation, mutation and methylation) from integrated analysis of three large-scale pharmacogenomic databases (GDSC, CellMiner and CCLE) [36].

3.16 Statistical analysis

All statistical analyses were performed using R software (version 4.1.2) and P values < 0.05 were considered statistically significant. The P values < 0.05, 0.01, and 0.001 were represented by *, **, and ***, respectively.

4. Results

4.1 Construction of prognostic risk assessment model for STAD

To screen out the genes related to prognosis of STAD, the study performed Lasso-penalized Cox regression analysis. According to the optimal λ (-3.5), we screened out 15 genes that were associated with overall survival (OS) in STAD patients, including GPX3, ADAMTS18, ASPA, CD36, SERPINE1, CYP19A1, LRAT, CGB5, BCHE, ANO3, SOX14, CYMP, CFHR4, F13B and OTX2 (Figure 1A, Figure S1A); Multivariate COX regression models were used to confirm that the 14 gene expression levels were negatively correlated with OS, while SOX14 mRNA expression levels was positively correlated with OS in STAD (Figure 1B). The study also constructed risk score model by Lasso-penalized Cox (Figure S1B-C), and evaluated the risk scores of STAD patients through Kaplan-Meier (KM) curves and receiver operating characteristic (ROC) curves.

The result indicated that the survival rate of the high-risk group was lower than that of the low-risk group (Figure 1C); moreover, the area under curve (AUC) of the model to predict the 1-, 3-, and 5-years survival rates of STAD patients were 0.67, 0.75, and 0.82, respectively (Figure 1D). These results help us to evaluate the correlation between the selected target genes and prognosis in a multi-dimensional manner.

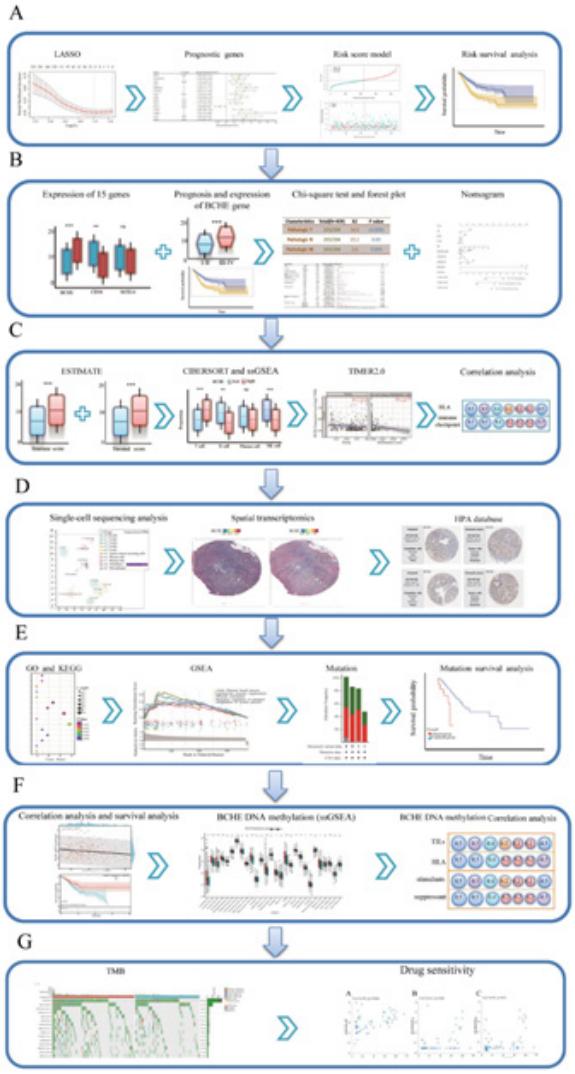

Scheme: Schematic diagram of the study design.

(A) Lasso-penalized Cox regression analysis was performed to construct STAD prognostic-related gene signatures, and screened out the target gene BCHE. (B) The correlation between BCHE mRNA expression level and clinicopathological information and prognosis of STAD were analyzed. (C) Next, the correlation between BCHE mRNA in STAD and immune infiltrating cells and immune reaction-related molecules through multiple databases and algorithms. (D) The single-cell sequencing and spatial transcriptomics analysis of BCHE. (E) Enrichment analysis and mutation analysis of BCHE mRNA. (E) Methylation analysis of BCHE mRNA. (F) Finally, Tumor Mutation Burden and drug sensitivity Analysis of BCHE mRNA.

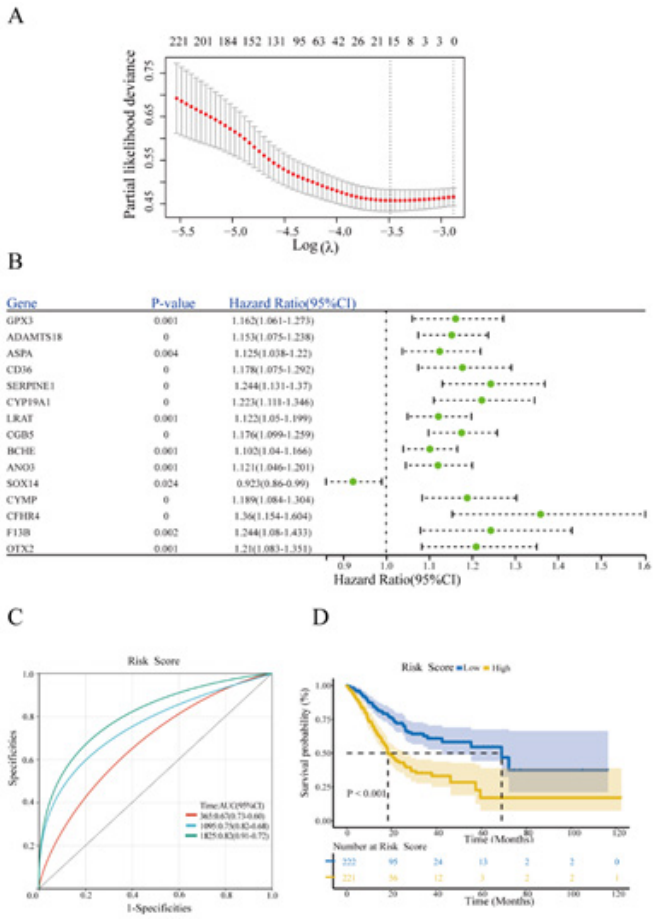

Figure 1: Construction of the prognostic risk model

(A) Lasso-penalized Cox regression analysis was performed to construct STAD prognostic-related gene signatures. The y-axis represents the partial likelihood deviance. The vertical line on the left represents the 15 genes used for model construction. (B) The forest plot represents the hazard ratio and 95% confidence interval for the 15 prognostic-related genes. (C) Time-dependent receiver operating characteristic (ROC) curves for the risk score in the STAD. (D) The Kaplan-Meier (KM) curves for the high- and low-risk score groups of STAD patients.

4.2 High expression of BCHE in advanced stage of STAD and its correlation with prognosis and clinicopathological information

The study compared the expression level of 15 prognostic genes in tumor tissues and paracancer tissues through TCGA-STAD database (n = 450) (Figure 2A), and found that BCHE mRNA levels were higher in advanced-stage STAD (stage III/IV) than in early-stage STAD (stage I/II) (P = 0.02) (Figure 2B). We further analyzed the prognosis effect of 15 genes in STAD through KM analysis (Figure S2), and found that STAD patients with high BCHE mRNA expression predicted poor prognosis (P = 0.003) (Figure 2C). These results encourage us to target BCHE, and further investigated the relationship of BCHE expression level with clinicopathological factors.

Next, the study used the clinicopathological information of STAD patients (n=409) in Xena database, and the mean age of patients was 65.12±10.64 [37] (Table 1). The result showed that high BCHE mRNA expression in tumor cells was associated with age (x^2 = 4.117, P = 0.041), T stage (x^2 = 8.338, P = 0.04), lymph node metastasis (x^2 = 13.412, P = 0.037), and tumor stage (x^2 = 28.007, P < 0.0001). There was no correlation with gender, distant metastasis, tumor stage, or *H. pylori* infection.

In order to study the prognostic value of BCHE, forest map and nomogram model were constructed in this study. Forest map results indicated that high BCHE mRNA expression group (HR = 1.74, P = 0.0001), > 65 years age (HR = 1.42, P = 0.02), without received radiation therapy (HR = 2.96, P = 0.006), without received target molecular therapy (HR = 1.44, P = 0.03), distant metastasis (HR = 2.21, P = 0.006), lymph node metastasis N1 (HR = 1.67, P = 0.03) / N2 (HR = 1.84, P = 0.01) / N3 (HR = 4.13, P < 0.001), and TNM stage III (HR = 2.27, P = 0.005) / IV (HR = 3.62, P < 0.001), is an independent risk factor for prognosis of STAD patients (Figure 2D). The results of the nomogram also confirmed the above views of forest map (Figure 2E).

Table 1: Association of BCHE mRNA expression with clinicopathologic information

Characteristics	BCHE low (%)	BCHE high (%)	Total (%)	x^2	pvalue
tumor grade				**28.007**	**<0.0001***
G1	6(1.47%)	6(1.47%)	12(2.93%)		
G2	90(22.00%)	54(13.20%)	144(35.21%)		
G3	104(25.43%)	140(34.23%)	244(59.66%)		
GX	4(0.98%)	5(1.22%)	9(2.20%)		
pathologic M				1.4	0.497
M0	182(44.50%)	181(44.25%)	363(88.75%)		
M1	11(2.69%)	16(3.91%)	27(6.60%)		
MX	11(2.69%)	8(1.96%)	19(4.65%)		
pathologic T				**13.412**	**0.037***
T1	16(3.91%)	5(1.22%)	21(5.13%)		
T2	30(7.33%)	35(8.56%)	65(15.89%)		
T2a+T2b	12(2.93%)	9(2.20%)	31(5.13%)		
T3	91(22.25%)	88(21.52%)	179(43.77%)		
T4	10(2.44%)	21(5.13%)	31(7.58%)		
T4a+T4b	43(10.51%)	40(9.78%)	83(20.29%)		
TX	2(0.49%)	7(1.71%)	9(2.20%)		
pathologic stage				3.051	0.384
Stage I	21(5.13%)	16(3.91%)	37(9.04%)		
Stage II	55(13.45%)	67(16.38%)	122(29.83%)		
Stage III	91(22.25%)	78(19.07%)	169(41.32%)		
Stage IV	19(4.63%)	22(5.38%)	41(10.01%)		
pathologic N				**8.338**	**0.04***
N0	64(15.65%)	55(13.45%)	119(29.10%)		
N1	45(11.00%)	66(16.14%)	111(27.14%)		
N2	48(11.74%)	31(7.58%)	79(19.32%)		
N3	40(9.78%)	42(10.27%)	82(20.05%)		
gender				1.143	0.285
FEMALE	78(19.07%)	68(16.63%)	146(35.70%)		
MALE	126(30.81%)	137(33.50%)	263(64.30%)		
age				**4.117**	**0.041***
<=65	55(13.45%)	76(18.58%)	131(32.03%)		
>65	149(36.43%)	129(31.54%)	278(67.97%)		
residual tumor				5.817	0.12
R0	170(44.62%)	156(40.94%)	326(85.56%)		
R1	5(1.31%)	11(2.89%)	16(4.20%)		
R2	9(2.36%)	8(2.10%)	17(4.46%)		
RX	7(1.84%)	15(3.94%)	22(5.78%)		

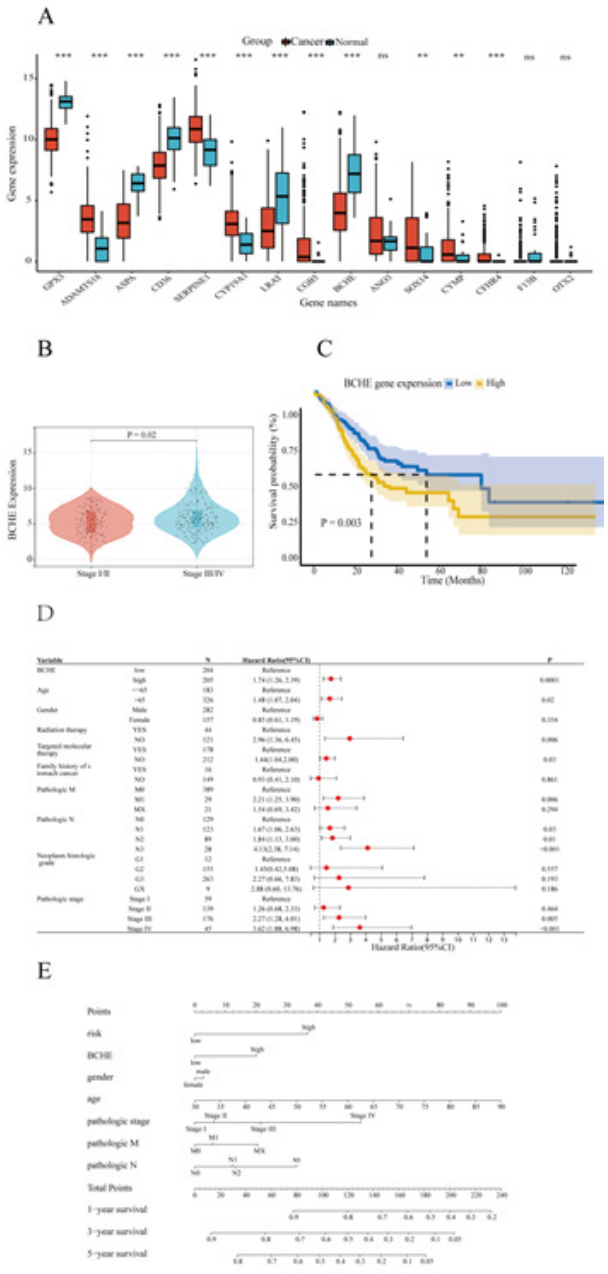

Figure 2: The expression and prognosis of BCHE mRNA in STAD, and establish forest chart and forecast nomogram

(A) Box plots showed the mRNA expression level of 15 prognostic genes in STAD tissues and paracancer tissues were compared. (B) BCHE mRNA expression level in STAD tissues at early (I/II) or advanced stages (III/IV). (C) Kaplan-Meier (KM) curves analysis was applied to evaluate the association of BCHE expression with the overall survival (OS) of STAD patients. (D) Forest chart of STAD multivariate cox analysis in the TCGA cohort. (E) The nomogram for predicting the proportion of STAD patients with 1-, 3-, or 5-year OS.

4.3 BCHE expression related with immune cells infiltration and immune reactivity related molecules in STAD

More and more evidences indicate that the infiltration of immune cells in TME plays an important role in regulating the occurrence, development and prognosis of STAD [38]. The study first used the ESTIMATE algorithm to score immune cells, stromal cells, and tumor purity in the TCGA-STAD samples (cut-off point set as 50% as report) [23], and found that BCHE expression was higher in the high-immune group ($P < 0.001$) (Figure 3A) and high-stromal groups ($P < 0.001$) (Figure S1D). These results suggested that the expression level of BCHE may be related to the infiltration of immune cells in the STAD microenvironment.

To investigate which types of immune cell infiltration are associated with BCHE expression, CIBERSORT and ssGSEA algorithms were used to calculate the proportion and expression of different immune cell types in TCGA-STAD tissues, respectively. The result showed that high BCHE expression was associated with multiple types of immune cell infiltration, including Plasma cells, B cell naive, B cell memory, CD4 memory resting, T cells regulatory, NK cell resting, Immature B cell, Immature dendritic cell, T cells follicular helper, Monocytes/ Monocytes M0/ Monocytes M2 and Mast cells resting/activated, Type 1/2/17 T helper cell, etc ($P < 0.05$) (Figure 3B-C). Next, the study used TIMER database to study the correlation between BCHE gene expression and immune cell infiltration. The results showed that BCHE is positively correlated with the infiltration of Mast cells (R=0.432, $P<0.001$), endothelial cell (R=0.414, $P<0.001$), Myeloid dendritic cell (R=0.467, $P<0.001$), Macrophage (R=0.546, $P<0.001$), Monocytes (R=0.338, $P<0.001$), and Cancer associated Fibroblast (R=0.75, $P<0.001$) in STAD; while negatively correlated with B cell plasma (R=-0.312, $P<0.001$), T cell $CD4^+$ Th1 (R=-0.469, $P<0.001$), Plasmacytoid dendritic cell (R=-0.302, $P<0.001$) (Figure 3D).

Finally, we studied the correlation between BCHE expression and HLA family genes and immune checkpoint, and the results showed that most HLA family genes and immune checkpoint genes were significantly positively correlated with BCHE gene expression (Figure 3E). In addition, BCHE has been found to be closely related to immune cell infiltration and immune reactivity related molecules in other tumor types (Figure S3A-D).

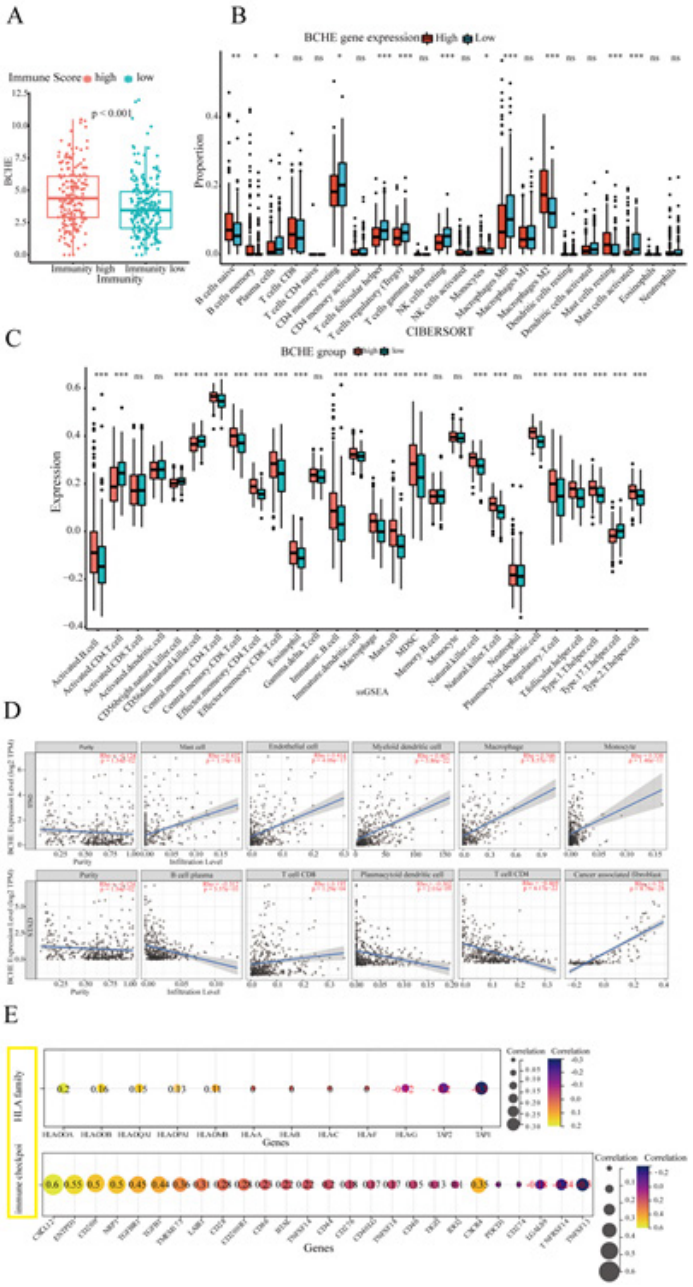

Figure 3: BCHE mRNA is closely related to immunity in STAD

(A) Comparison of immune scores between the high- and low-immune group based on ESTIMATE. (B) Comparison of immune cells infiltration between high- and low-BCHE mRNA group (CIBERSORT). (C) Comparison of immune cells infiltration between high- and low-BCHE mRNA group (ssGSEA). (D) TIMER analysis of purity-corrected partial Spearman's correlation between the expression of BCHE and various immune cells in STAD. (E) Correlation analysis for expression of BCHE mRNA and expression of immune checkpoints and HLA family genes. The P values are labeled using asterisks (ns, no significance, *P < 0.05, **P < 0.01, ***P < 0.001).

4.4 Cell-specific and tissue-specific analysis of BCHE expression

To investigate the cell specificity of BCHE expression, single-cell sequencing results from the HPA database were used in this study. The single-cell analysis showed that the BCHE gene was mainly expressed in fibroblasts of gastric tissue (44.6 nTPM) (Figure 4A). Next, The lollipop plot results showed that BCHE mRNA was mainly expressed in gastric cancer cell lines ECC12, HS764T, HGC27 in CCLE database (Figure 4B).

The HPA database and 10 × Genomics Visium platform were further used to detect the tissue specificity of BCHE expression in STAD patients. The IHC images showed that BCHE was highly stained in gastric cancer, but low in normal gastric tissue (Figure 4C); meanwhile BCHE gene was significantly expressed in tumor tissue through spatial transcriptome analysis (Figure 4D).

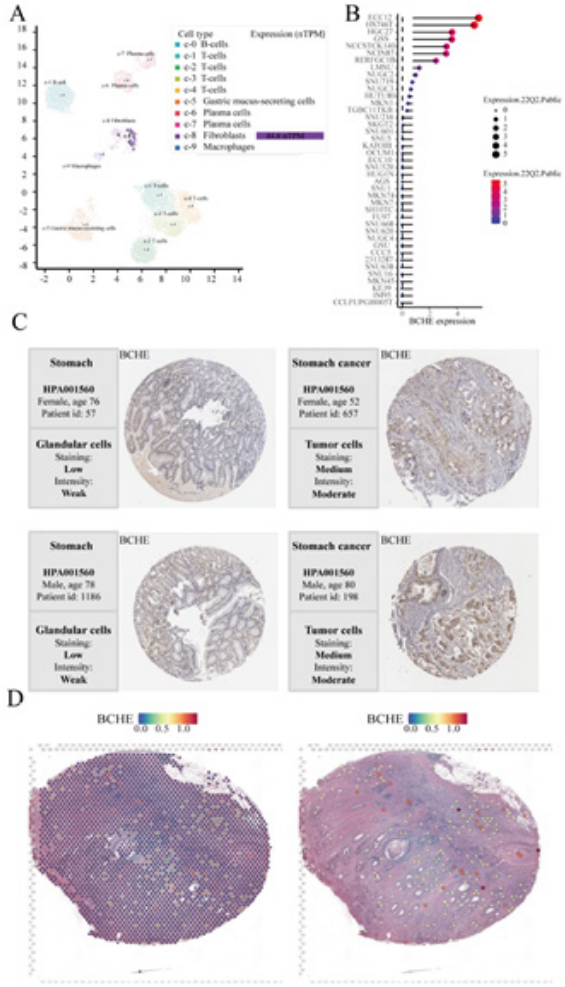

Figure 4: Cell-specific and tissue-specific analysis of BCHE expression

(A) UMAP plot depicting nine cell clusters and the distribution of BCHE mRNA expression levels within the nine cell clusters. (B) Lollipop chart showing the expression of BCHE mRNA on gastric cancer cell lines. (C). IHC images of BCHE in gastric cancer and normal tissues detected in the HPA database. (D) Left panels: Spot plots depicting log-transformed normalized expression (logcounts) for gene BCHE; Right panels: the corresponding histology slide.

4.5 The regulatory mechanism and mutation type of BCHE in STAD

To further understand the regulatory mechanism of BCHE, some genes related to BCHE function were enriched by DAVID database and R software , including CHAT, PRIMA1, COLQ, APP, GPT ($P < 0.05$) (Figure S1E). The result showed that these genes were most associated with positive regulation of apoptotic process, negative regulation of cell proliferation, positive regulation of MAPK cascade, extracellular region and identical protein binding by gene ontology (GO) analysis (Figure 5A); moreover, over expression these genes were involved in Alzheimer's disease, Serotonergic synapse, multiple amino acid metabolism, and drug metabolism - cytochrome P450 by kyoto encyclopedia of genes and genomes KEGG) analysis (Figure 5B). Further GSEA (Gene Set Enrichment Analysis) analysis showed that the signaling pathways of the BCHE high expression group were mainly distributed in actin filament based process, actomyosin structure organization, muscle contraction, negative regulation of transport and regulation of system process (Figure 5C), while the signaling pathways of the BCHE low expression group were mainly distributed in antimicrobial humoral response, meiotic cell cycle, antimicrobial humoral response, meiotic cell cycle, organic anion transmembrane transporter activity, orgain hydroxy compound catabolic process, sister chromatid segregation (Figure 5D).

To better understand the function of BCHE gene, the mutated form and relationship with prognosis in STAD were further analyzed through cBioPortal database. The analysis result showed that BCHE mutation occurred in about 30 of 295 patients with STAD, and the mutation rate was 10.17% (Figure 5E), and the two main forms of mutation were amplification (50.00%) and mistranslation (27.27%) (Figure S1F). The KM curve indicated that the OS of the BCHE mutation group was lower than that of the BCHE wild type group ($P = 0.0186$) (Figure 5F), and the OS of the amplification group was also lower than that of the BCHE wild-type group ($P = 0.04$) (Figure 5G).

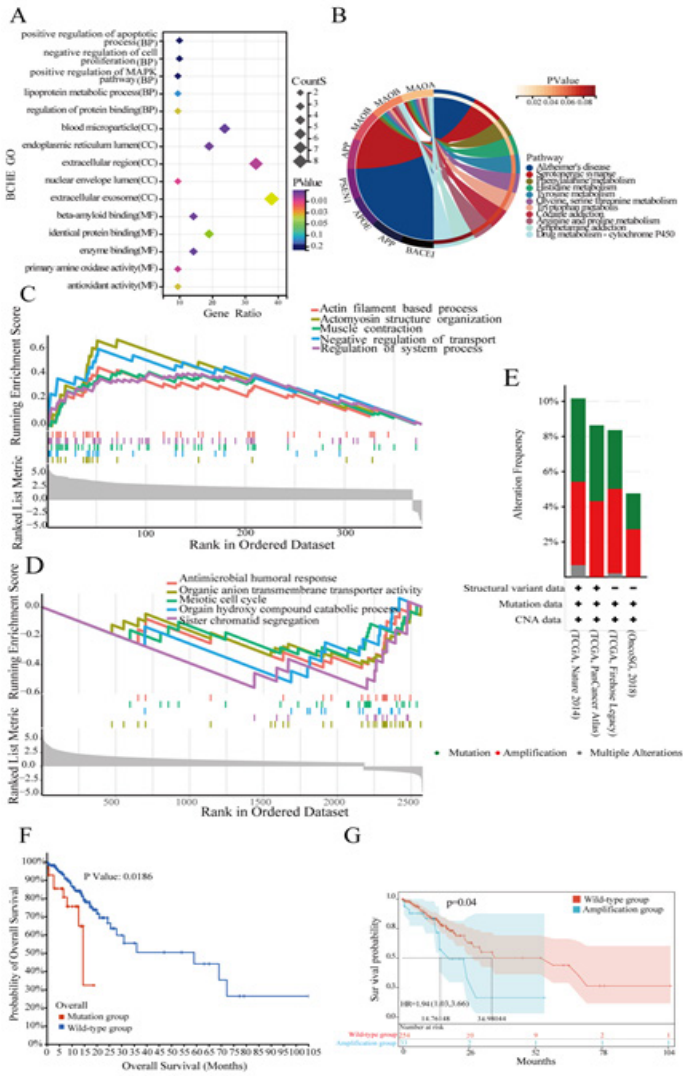

Figure 5: Enrichment analysis and mutation analysis of BCHE mRNA

(A) GO enrichment plot of the top 20 genes with the highest correlation with BCHE. (B) KEGG enrichment plot of the top 20 genes with the highest correlation with BCHE. (C) Gene Set Enrichment Analysis of BCHE high expression group. (D) Gene Set Enrichment Analysis of BCHE low expression group. (E) Mutation rate of BCHE in STDA patients was analyzed using the cBioPortal online tool. (F) The Kaplan-Meier (KM) curves for the mutation group and wild type group of BCHE mRNA. (G) The Kaplan-Meier (KM) curves for the amplification group and wild type group of BCHE mRNA.

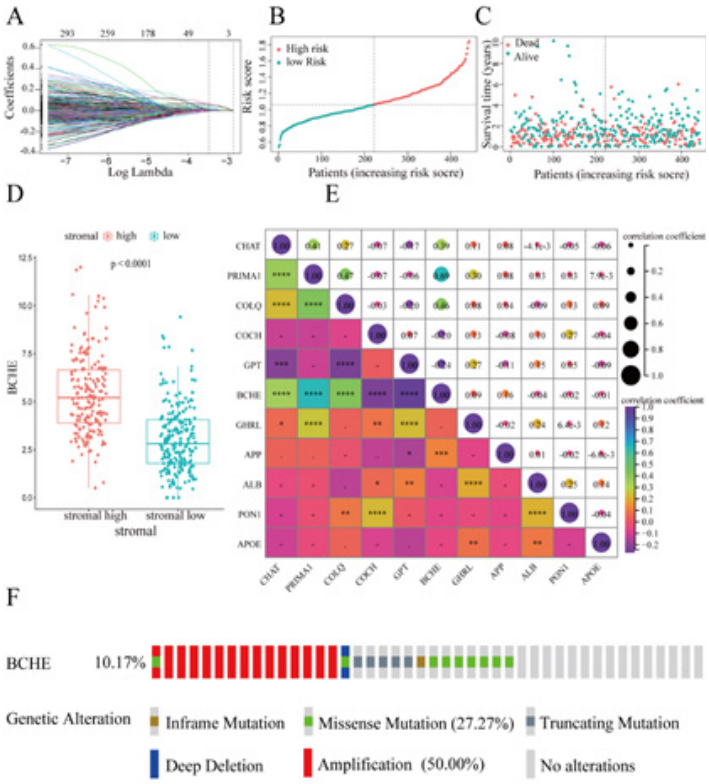

Figure S1: (A) LASSO regression analysis was performed to construct STAD prognostic-related gene signatures. (B-C) Distribution of risk scores of high- and low-risk STAD patients based on 15 genes prognostic signature. (D) Comparison of stromal scores between the high- and low- stromal group based on ESTIMATE. (E) Correlation matrix plot of BCHE genes and the 10 most correlated genes. (F) Mutation type of BCHE in STDA patients was analyzed using the cBioPortal online tool.

4.6 Methylation analysis of BCHE mRNA

To further investigate the relationship between DNA methylation and BCHE mRNA expression, we found a significant negative correlation between BCHE mRNA expression and BCHE DNA methylation through cBioPortal database analysis ($R = -0.17$, $p < 0.01$) (Figure 6A). The KM curve indicated that the OS of the BCHE hypermethylated group was lower than that of the BCHE hypomethylated group ($P = 0.03$) (Figure 6B). Next, we investigated the correlation between BCHE DNA methylation and immune cell infiltration. The result showed that high BCHE DNA methylation was associated with multiple types of immune cell infiltration, including activated B cell, activated CD4/CD8 T cell, activated dendritic cell, central memory CD4 T cell, effector memeory CD8 T cell, immature B cell, MDSC, monocyte, natural killer cell, type 1 T helper cell ($P < 0.05$) (Figure 6C). Finally, we analyzed the association of BCHE DNA methylation with immune cells, HLA family genes and immune checkpoints through the TISIBD database., and the results showed that most immune cells, HLA family genes and immune checkpoints were significantly positively correlated with BCHE DNA methylation (Figure 6D-G).

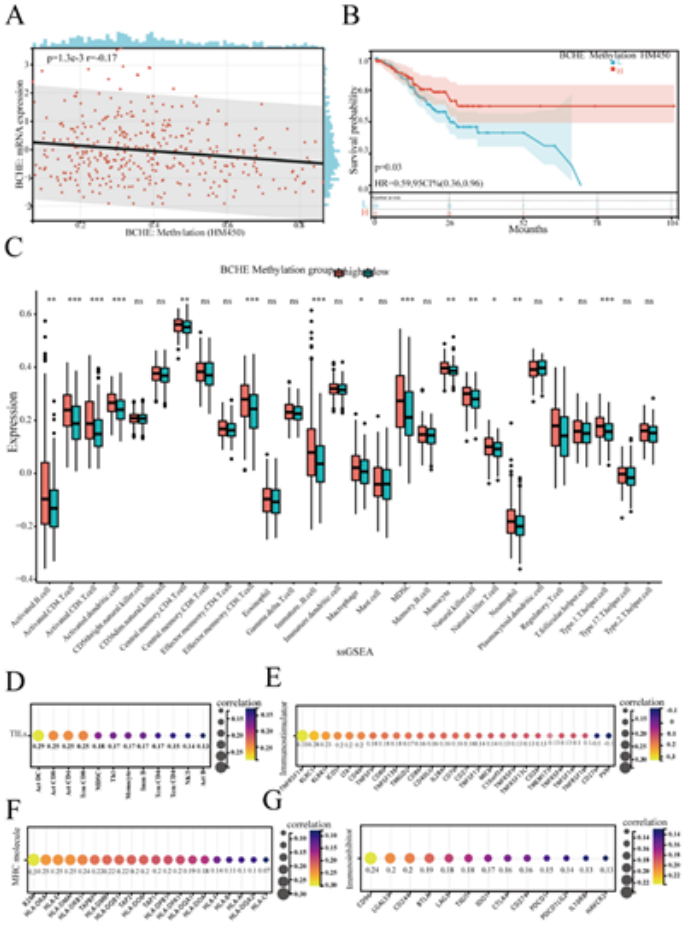

Figure 6: Methylation analysis of BCHE mRNA

(A) The expression of BCHE mRNA was negatively regulated by DNA methylation. (B) KM curves analysis was applied to evaluate the association of BCHE DNA methylation with the overall survival (OS) of STAD patients. (C) Comparison of immune cells infiltration between high- and low-BCHE methylation group (ssGSEA). (D-G) Correlation analysis for expression of BCHE DNA methylation and expression of tumor infiltrating lymphocytes (TILs), immune checkpoints and HLA family genes. The P values are labeled using asterisks (ns, no significance, *P < 0.05, **P < 0.01, ***P < 0.001).

4.7 The significance of BCHE expression in clinical treatment

To further investigate the role of BCHE in guiding clinical treatment, 15 genes with the highest frequency of mutations in STAD were selected, including TTN (68.2%), MUC16 (41.5), DNAHI1 (18.0%), USH2A (17.7%), NBEA (16.7%), RYR3 (16.1%), KMT2C (15.8%), MDN1 (15.8%), NEB (15.8), PTPRT (15.1%), RIMS2 (14.8%), MACF (13.8%), NRXN1 (13.5%)), DCLK1 (13.5%), PEG3 (13.2%) (Figure 7A). Then combined with the expression level of BCHE, they were divided into high- and low- expression group. The result indicated that the TMB (tumor mutational burden) score of the high BCHE expression group was lower than that of low BCHE expression group ($P < 0.01$) (Figure 7B). The KM survival curve results showed that survival rate of the high-TMB group was better than that of the low-TMB group ($P = 0.04$) (Figure 7C).

Next, we further investigated the potential correlation between drug sensitivity and BCHE expression using the RNAactDrug database. The expression of BCHE was associated with the drug sensitivity of Asaley (R=0.401, P<0.001), Dabrafenib (R=0.379, *P*<0.001) and Vemurafenib (R=0.394, P<0.001) (Figure 7D-F). In addition, the expression of BCHE is also related to the drug sensitivity of crotoxin cd, sb-476429-a, sb-682330-a, 1,6-bis [4- (4-aminophenoxy) phenyl] diamantane, hydrogeldanamycin-18,21-diacetate, benzo [b] naphtho [2,3-d] furan- 6,11 -dione, 4-chloro-3-hydroxy, protein toxin a 23 - mw approx. 6700, riboprine(usan) and sb-610251-b (Figure S4A-I).

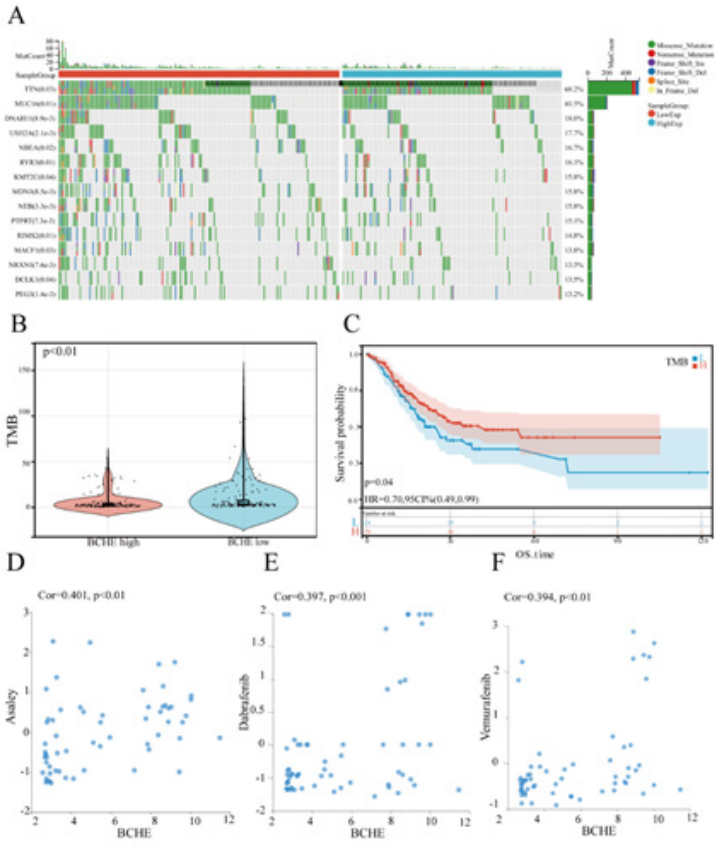

Figure 7: Tumor Mutation Burden and Drug Sensitivity Analysis of BCHE

(A) Waterfall chart showing the difference of frequently mutated genes between high-/low- BCHE expression groups. The left panel shows the genes ordered by their mutation frequencies. The right panel presents different mutation types. (B) Difference of TMB between patients from the low-/high-BCHE expression. (C) The Kaplan-Meier (KM) curves for the high- and low-TMB score groups of STAD patients. (D-F) Effect of different expression levels of BCHE on drug sensitivity, the expression of BCHE was associated with the sensitivity of Asaley, Dabrafenib and Vemurafenib.

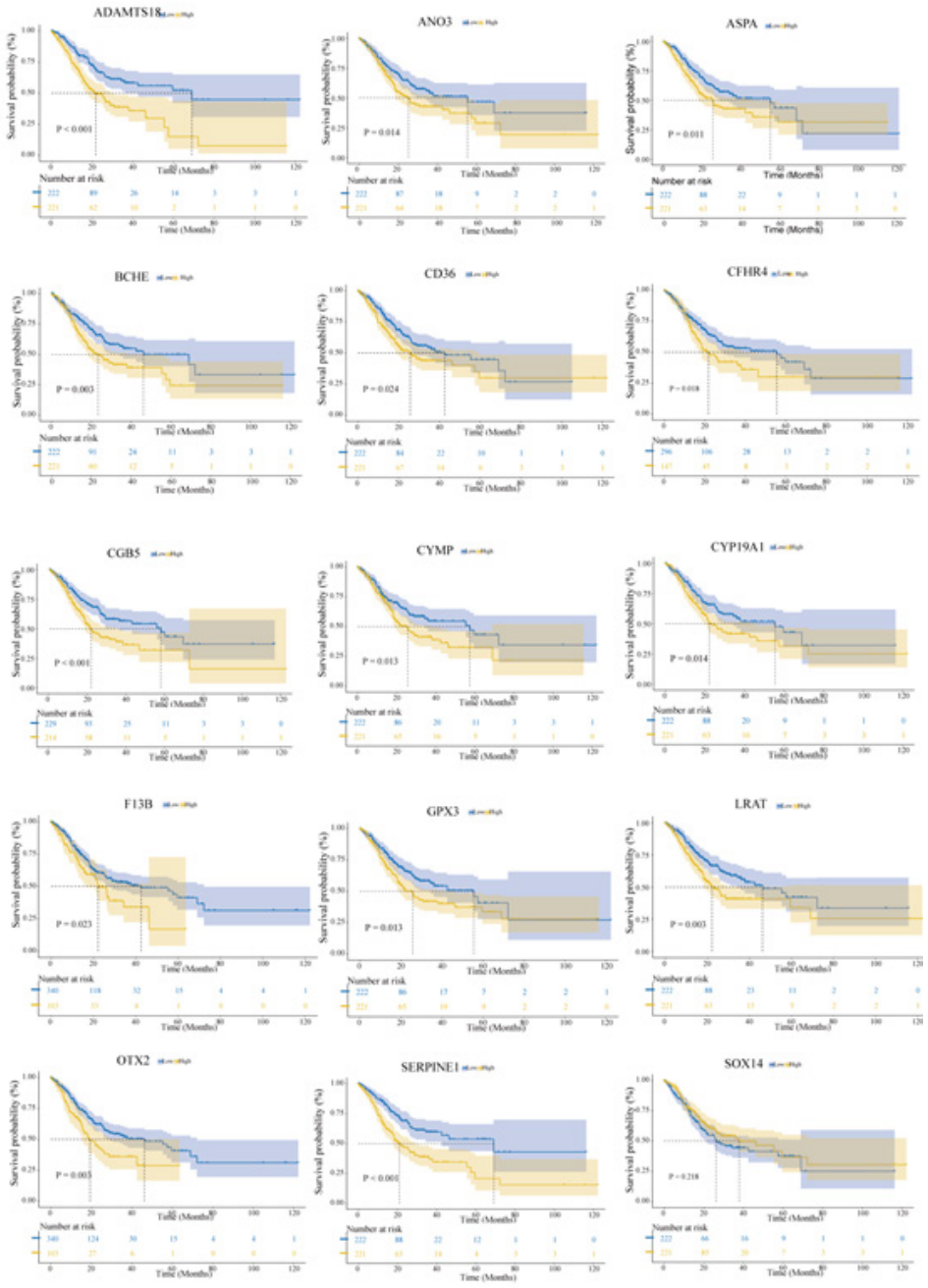

Figure S2: Kaplan–Meier survival curve analysis verified the prognostic value of 15 genes in STAD.

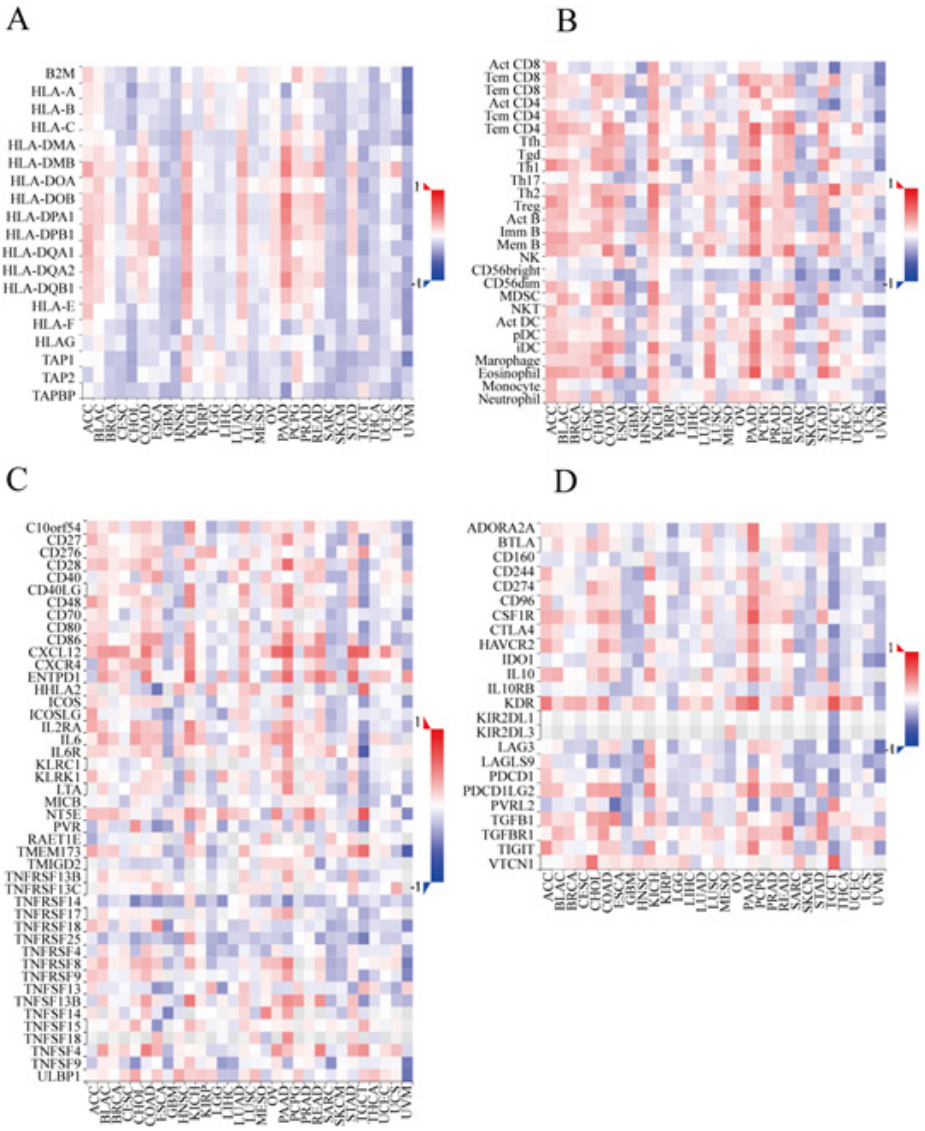

Figure S3: (A) The heatmap showed the correlation between BCHE and MHC molecules in various cancers. (B) The heatmap showed the correlation between BCHE and immune cells in various cancers. (C) The heatmap showed the correlation between BCHE and immunostimulators in various cancers. (D) The heatmap showed the correlation between BCHE and immunoinhibitors in various cancers. The plot above were downloaded from http://cis.hku.hk/TISIDB/.

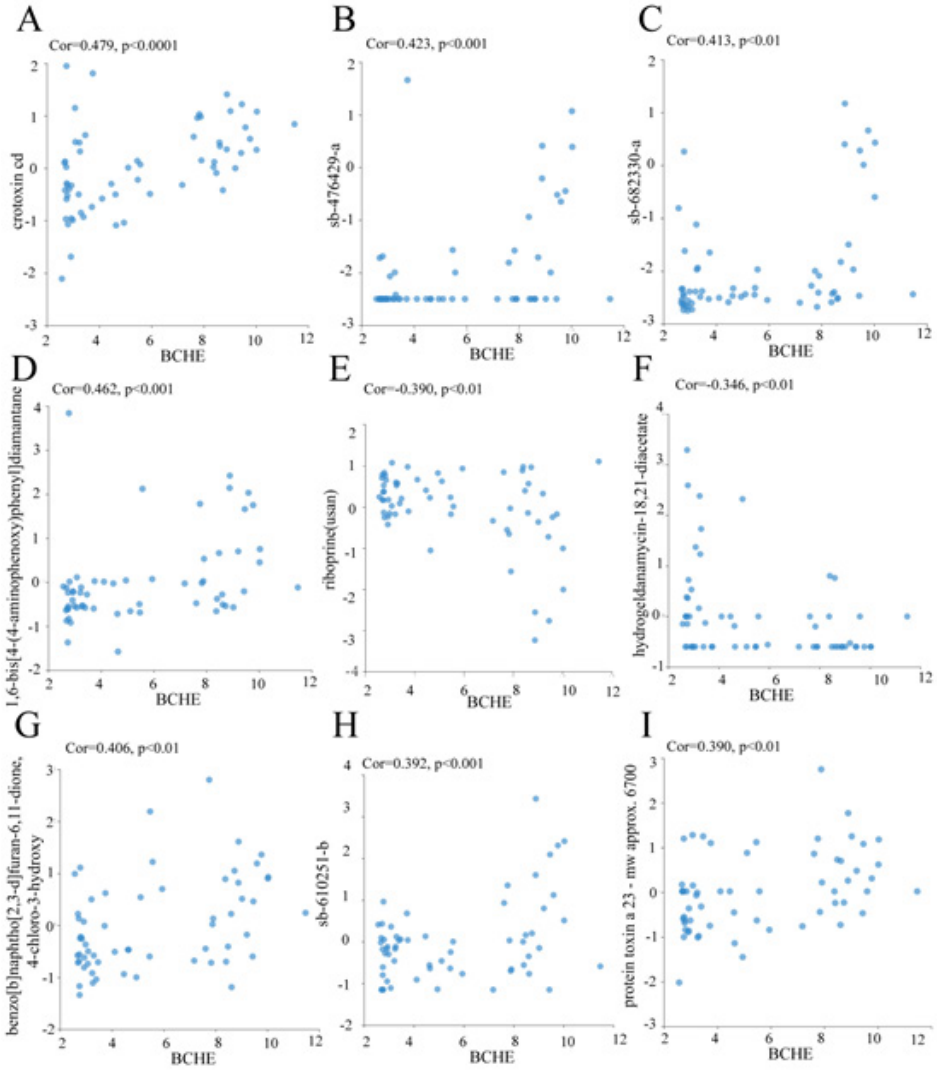

Figure S4: Effect of different expression levels of BCHE on drug sensitivity. The expression of BCHE was associated with the sensitivity of crotoxin cd (A), sb-476429-a (B), sb-682330-a (C), 1,6-bis [4- (4-aminophenoxy) phenyl] diamantane (D), riboprine(usan) (E), hydrogeldanamycin-18,21-diacetate (F), benzo[b]naphtho[2,3-d]furan-6,11-dione, 4-chloro-3-hydroxy (G), sb-610251-b (H), protein toxin a 23 - mw approx. 6700 (I).

5. Discussion

Existing studies found that BCHE may be involved in the regulation of cell apoptosis, cell differentiation and proliferation, cell adhesion and tumorigenesis [39, 40]. Therefore, BCHE may be used as a potential biomarker for cancer diagnosis [10]. However, the expression level of BCHE in different tumors is not consistent. For example, BCHE expression is low in endometrial cancer and colorectal cancer [41, 42], but high in ovarian cancer, breast cancer, and some lung squamous cell carcinomas [43-45]. In addition, BCHE is down-regulated in the early stage of prostate cancer and up-regulated in the late stage [15]. This indicates that BCHE plays different regulatory roles in different tumors, even in different stages of the same tumor. In this study, we found that BCHE mRNA was highly expressed in patients with advanced STAD and was associated with poor prognosis. In addition, high expression of BCHE mRNA can promote the infiltration of immune cells in the tumor microenvironment of gastric cancer. Therefore, this study aims to explore the expression and regulation mechanism of BCHE in STAD.

In this study, we first studied the expression of BCHE mRNA in STAD, and the results showed that compared with early STAD, the expression level of BCHE mRNA in patients with advanced STAD was significantly increased. In addition, prognostic analysis showed that STAD patients with high BCHE mRNA expression had a poor prognosis. It has been reported that BCHE is also a prognostic biomarker for a variety of cancers. For example, the expression of BCHE mRNA in prostate cancer is bipolar, that is, decreased in early stage and increased in late stage. Prostate patients with high expression of BCHE mRNA have a poor prognosis [15].In addition, high BCHE mRNA expression was associated with decreased OS in lung [46], ovarian [45], and head and neck squamous cell carcinomas [47].

ESTIMATE, CIBERSORT and ssGSEA are three common algorithms to investigate the relationship between gene expression and immune cell infiltration in the tumor microenvironment. Each has its own advantages and disadvantages: The ESTIMATE algorithm

can estimate tumor purity, immune cell and stromal cell scores, but cannot give specific ratios or values for each cell [48]; CIBERSORT algorithm is used to estimate the proportion of 22 immune cell subtypes in cancer tissues, but the value of the proportion is not the actual value [49]; SsGSEA algorithm is based on the single sample gene enrichment analysis (ssGSEA) method to calculate the infiltration degree of 28 immune cell subtypes, so it is prone to deviation [25, 50].

In the study, we used the ESTIMATE algorithm to find that BCHE mRNA expression was higher in the high-immune score group and high-stromal cell group of STAD, suggesting that BCHE is closely related to TME of STAD. CIBERSORT and ssGSEA algorithm results showed that BCHE mRNA expression was significantly positively correlated with monocytes, endothelial cells, cancer-associated fibroblasts, mast cells and macrophages in STAD, and BCHE was positively correlated with the expression of most immune biomarkers in STAD. These results suggest that BCHE may play an important role in the STAD immune microenvironment.

Different monocyte subsets play different functions in TME [51]. For example, endothelial cells, in addition to providing nutrients to tumor tissue, act as cancer niche cells and create an environment that promotes cancer; Mast cells play a carcinogenic role in STAD by releasing lymphangiogenic factors (VEGF-F and VEGF-C) and angiogenic factors (CXCL8, VEGF-A and MMP-9) [52]. Macrophages promote the migration and invasion of STAD cells by stimulating the expression of VEGF and MMP-9 [53]. In this study, BCHE mRNA was significantly correlated with cancer-associated fibroblasts (CAFs) ($R = 0.75$, $P < 0.001$). CAFs is one of the most important stromal cell types in TME, and various growth factors, cytokines and chemokines secreted by CAFs in STAD constitute a favorable environment for inducing tumor growth, invasion and migration [54].These results support that BCHE can promote the disease progression of STAD by regulating the function of immune cells in the TME.

The results of single-cell sequencing analysis found that BCHE mRNA was mainly enriched in fibroblasts, which is consistent with the results of tumor immune infiltration analysis in the study. CAF is the most abundant cell type in TME, and also the center of cross-communication between various cells in tumor stroma. A large number of CAFs in tumor tissue constitute a good environment for tumor development [55]. CAFs communicate with other stromal cells and tumor cells by secreting various cytokines, inhibit immune cell function, and promote tumor development, invasion and metastasis [56]. For example, the secretion of vascular endothelial growth factor (VEGF) can regulate tumor blood vessels; Secreted TGF-β inhibited DC maturation and promoted Treg differentiation; Secreted interleukin-6 (IL-6) promotes MDSC differentiation and inhibits cytotoxic T cells. Activated CAF also secretes chemokines (CXCL12 and CXCL14) to promote tumor development [57]. In addition, CAFs promote the solidification of tumor extracellular matrix by secreting a large amount of collagen and fibronectin, and form a penetration barrier of drug or therapeutic immune cells, which prevents the penetration of drugs and immune cells into the deep layer of tumor tissue, thus reducing the therapeutic effect of tumor [55, 58, 59]. Our study showed that BCHE can participate in the regulation of cell migration, invasion and proliferation, but whether it can promote the migration, invasion and proliferation of tumor cells by regulating the function of CAFs remains to be confirmed in the next step.

The enrichment results of this study found that the regulation mechanism of BCHE may be related to positive regulation of apoptotic process, negative regulation of cell proliferation, positive regulation of MAPK cascade, and extracellular region and identical protein binding. Cholinesterase (CHE) contains acetylcholinesterase (ACHE) and butyylcholinesterase (BCHE), which are 65% homologous in amino acid sequence [60]. Although the role of CHE in tumors is unclear, overexpression of CHE has been shown to promote apoptosis and inhibit cell proliferation [16, 40], and studies have shown that CHE inhibits cell proliferation through nicotinic and muscarinic receptor-mediated mechanisms [61].In addition, CHE can also act as a cell-matrix or cell-cell adhesion molecule [62].

Finally, another important finding in this study is that the total mutation rate of BCHE mRNA in STAD was as high as 10.17%, in which the amplification mutation accounted for 50.00%, and the OS of both the BCHE mutation group and the amplification mutation group was lower than that of the BCHE wild-type group. BCHE mRNA mutations will lead to various genotypes and phenotypes, such as H, J and K type mutants, which will lead to a decrease in enzyme activity; while Johannesburg, $C5^+$ and Cynthiana mutants will lead to an increase in enzyme activity [63-65]. Studies have also shown that mutations of BCHE mRNA mainly occur in diseases such as Alzheimer's disease [66], coronary heart disease [67], childhood mental retardation [68] and tumors [62]. Therefore, the high expression of BCHE mRNA in STAD patients may be related to BCHE mRNA amplified mutations, which leading to poor prognosis of patients.

6. Conclusion

BCHE as a prognostic biomarker for STAD, and the regulatory mechanism of BCHE might be related with its function in cell proliferation, differentiation and other related signaling pathways.

7. Acknowledgments

The study was supported by the National Natural Science Foundation of China, (82273196, 32060018); Special fund projects for guide local science and technology development by the China government (GUIKEZY20198004).

References

1. Sung H, Ferlay J, Siegel RL, Laversanne M, Soerjomataram I, Jemal A, et al. Global Cancer Statistics 2020: GLOBOCAN Estimates of Incidence and Mortality Worldwide for 36 Cancers in 185 Countries. CA: a cancer journal for clinicians. 2021; 71: 209-49.
2. Zhao W, Jia L, Zhang M, Huang X, Qian P, Tang Q, et al. The killing effect of novel bi-specific Trop2/PD-L1 CAR-T cell targeted gastric cancer. American journal of cancer research, 2019; 9 :1846-56.
3. Xia C, Dong X, Li H, Cao M, Sun D, He S, et al. Cancer statistics in China and United States, 2022: profiles, trends, and determinants. Chinese medical journal, 2022; 135: 584-90.
4. Rawla P, Barsouk A. Epidemiology of gastric cancer: global trends, risk factors and prevention. Przeglad gastroenterologiczny, 2019; 14: 26-38.
5. Saito H, Fukumoto Y, Osaki T, Fukuda K, Tatebe S, Tsujitani S, et al. Distinct recurrence pattern and outcome of adenocarcinoma of the gastric cardia in comparison with carcinoma of other regions of the stomach. World journal of surgery, 2006; 30: 1864-9.
6. Wagner AD, Syn NL, Moehler M, Grothe W, Yong WP, Tai BC, et al. Chemotherapy for advanced gastric cancer. The Cochrane database of systematic reviews, 2017; 8: Cd004064.
7. Allemani C, Matsuda T, Di Carlo V, Harewood R, Matz M, Nikšić M, et al. Global surveillance of trends in cancer survival 2000-14 (CONCORD-3): analysis of individual records for 37 513 025 patients diagnosed with one of 18 cancers from 322 population-based registries in 71 countries. Lancet (London, England), 2018; 391: 1023-75.
8. Chatonnet A, Lockridge O. Comparison of butyrylcholinesterase and acetylcholinesterase. The Biochemical journal, 1989; 260: 625-34.
9. Gaughan G, Park H, Priddle J, Craig I, Craig S. Refinement of the localization of human butyrylcholinesterase to chromosome 3q26.1-q26.2 using a PCR-derived probe. Genomics, 1991; 11: 455-8.
10. Santarpia L, Grandone I, Contaldo F, Pasanisi F. Butyrylcholinesterase as a prognostic marker: a review of the literature. Journal of cachexia, sarcopenia and muscle, 2013; 4: 31-9.
11. Ostergaard D, Viby-Mogensen J, Hanel HK, Skovgaard LT. Half-life of plasma cholinesterase. Acta anaesthesiologica Scandinavica, 1988; 32: 266-9.
12. Paes AM, Carniatto SR, Francisco FA, Brito NA, Mathias PC. Acetylcholinesterase activity changes on visceral organs of VMH lesion-induced obese rats. The International journal of neuroscience, 2006; 116: 1295-302.
13. Cucuianu M, Nistor T, Hâncu N, Orbai P, Muscurel C, Stoian I. Serum cholinesterase activity correlates with serum insulin, C-peptide and free fatty acids levels in patients with type 2 diabetes. Romanian journal of internal medicine = Revue roumaine de medecine interne, 2002; 40: 43-51.
14. Kutty KM, Payne RH. Serum pseudocholinesterase and very-low-density lipoprotein metabolism. Journal of clinical laboratory analysis, 1994; 8: 247-50.
15. Gu Y, Chow MJ, Kapoor A, Mei W, Jiang Y, Yan J, et al. Biphasic Alteration of Butyrylcholinesterase (BChE) During Prostate Cancer Development. Translational oncology, 2018; 11: 1012-22.
16. Nair KK, Pramod GV, Chaudhuri K, Ashok L. Estimation of Serum Butyryl Cholinesterase in Patients with Oral Squamous Cell Carcinoma: A Cross-Sectional Study. Journal of clinical and diagnostic research : JCDR, 2017; 11: Zc59-zc62.
17. Klocker EV, Barth DA, Riedl JM, Prinz F, Szkandera J, Schlick K, et al. Decreased Activity of Circulating Butyrylcholinesterase in Blood Is an Independent Prognostic Marker in Pancreatic Cancer Patients. Cancers, 2020; 12.
18. Poetsch N, Sturdza A, Aust S, Polterauer S, Grimm C, Schwameis R, et al. The value of pretreatment serum butyrylcholinesterase level as a novel prognostic biomarker in patients with cervical cancer treated with primary (chemo-)radiation therapy. Strahlentherapie und Onkologie : Organ der Deutschen Rontgengesellschaft, 2019; 195: 430-40.
19. Goldman MJ, Craft B, Hastie M, Repečka K, McDade F, Kamath A, et al. Visualizing and interpreting cancer genomics data via the Xena platform. Nature biotechnology, 2020; 38: 675-8.
20. Zou C, Huang D, Wei H, Wu S, Song J, Tang Z, et al. Identification of Immune-Related Risk Signatures for the Prognostic Prediction in Oral Squamous Cell Carcinoma. Journal of Immunology Research, 2021; 203759.
21. Qi X, Wang R, Lin Y, Yan D, Zuo J, Chen J, et al. A Ferroptosis-Related Gene Signature Identified as a Novel Prognostic Biomarker for Colon Cancer. Frontiers in genetics, 2021; 12:692426.
22. He W, Wang B, He J, Zhao Y, Zhao W. SSR4 as a prognostic biomarker and related with immune infiltration cells in colon adenocarcinoma. Expert review of molecular diagnostics, 2022; 22: 223-31.
23. Zhang C, Zheng JH, Lin ZH, Lv HY, Ye ZM, Chen YP, et al. Profiles of immune cell infiltration and immune-related genes in the tumor microenvironment of osteosarcoma. Aging, 2020; 12: 3486-501.
24. Jiang S, Zhang Y, Zhang X, Lu B, Sun P, Wu Q, et al. GARP Correlates With Tumor-Infiltrating T-Cells and Predicts the Outcome of Gastric Cancer. Frontiers in immunology, 2021; 12: 660397.
25. Hänzelmann S, Castelo R, Guinney J. GSVA: gene set variation analysis for microarray and RNA-seq data. BMC bioinformatics, 2013; 14: 7.
26. Li T, Fu J, Zeng Z, Cohen D, Li J, Chen Q, et al. TIMER2.0 for analysis of tumor-infiltrating immune cells. Nucleic acids research, 2020; 48: W509-w14.
27. Ru B, Wong CN, Tong Y, Zhong JY, Zhong SSW, Wu WC, et al. TISIDB: an integrated repository portal for tumor-immune system interactions. Bioinformatics, 2019; 35: 4200-2.
28. Szklarczyk D, Gable AL, Nastou KC, Lyon D, Kirsch R, Pyysalo S, et al. The STRING database in 2021: customizable protein-protein networks, and functional characterization of user-uploaded gene/measurement sets. Nucleic acids research, 2021; 49: D605-d12.
29. Uhlén M, Fagerberg L, Hallström BM, Lindskog C, Oksvold P, Mardinoglu A, et al. Proteomics. Tissue-based map of the human proteome. Science (New York, NY), 2015; 347: 1260419.
30. 10x Genomics sequences in situ. Nature biotechnology, 2020; 38(11):1222.
31. Ghandi M, Huang FW, Jané-Valbuena J, Kryukov GV, Lo CC, McDonald ER, 3rd, et al. Next-generation characterization of the Cancer Cell Line Encyclopedia. Nature, 2019; 569: 503-8.

32. Sherman BT, Hao M, Qiu J, Jiao X, Baseler MW, Lane HC, et al. DAVID: a web server for functional enrichment analysis and functional annotation of gene lists (2021 update). Nucleic acids research. 2022; 23; 50: W216-W221.

33. Subramanian A, Tamayo P, Mootha VK, Mukherjee S, Ebert BL, Gillette MA, et al. Gene set enrichment analysis: a knowledge-based approach for interpreting genome-wide expression profiles. Proceedings of the National Academy of Sciences of the United States of America, 2005; 102: 15545-50.

34. Hu J, Yu A, Othmane B, Qiu D, Li H, Li C, et al. Siglec15 shapes a non-inflamed tumor microenvironment and predicts the molecular subtype in bladder cancer. Theranostics, 2021; 11: 3089-108.

35. Gao J, Aksoy BA, Dogrusoz U, Dresdner G, Gross B, Sumer SO, et al. Integrative analysis of complex cancer genomics and clinical profiles using the cBioPortal. Sci Signal. 2013; 2: 6 (269): pl1.

36. Dong Q, Li F, Xu Y, Xiao J, Xu Y, Shang D, et al. RNAactDrug: a comprehensive database of RNAs associated with drug sensitivity from multi-omics data. Brief Bioinform, 2020; 21(6):2167-74.

37. Jiang F, Wang XY, Wang MY, Mao Y, Miao XL, Wu CY, et al. An Immune Checkpoint-Related Gene Signature for Predicting Survival of Pediatric Acute Myeloid Leukemia. J Oncol, 2021; 5550116.

38. Ren N, Liang B, Li Y. Identification of prognosis-related genes in the tumor microenvironment of stomach adenocarcinoma by TCGA and GEO datasets. Biosci Rep, 2020; 30: 40(10).

39. Wessler I, Kirkpatrick CJ, Racké K. Non-neuronal acetylcholine, a locally acting molecule, widely distributed in biological systems: expression and function in humans. Pharmacol Ther. 1998; 77(1): 59-79.

40. Montenegro MF, Ruiz-Espejo F, Campoy FJ, Muñoz-Delgado E, de la Cadena MP, Rodríguez-Berrocal FJ, et al. Cholinesterases are down-expressed in human colorectal carcinoma. Cellular and molecular life sciences. CMLS. 2006; 63(18):2175-82.

41. Montenegro MF, Ruiz-Espejo F, Campoy FJ, Muñoz-Delgado E, de la Cadena MP, Cabezas-Herrera J, et al. Acetyl- and butyrylcholinesterase activities decrease in human colon adenocarcinoma. Journal of molecular neuroscience : MN, 2006; 30(1-2): 51-4.

42. Liu J, Tian T, Liu X, Cui Z. BCHE as a Prognostic Biomarker in Endometrial Cancer and Its Correlation with Immunity. J Immunol Res, 2022:6051092.

43. Brass N, Rácz A, Heckel D, Remberger K, Sybrecht GW, Meese EU. Amplification of the genes BCHE and SLC2A2 in 40% of squamous cell carcinoma of the lung. Cancer research, 1997; 57(11):2290-4.

44. Bernardi CC, Ribeiro Ede S, Cavalli IJ, Chautard-Freire-Maia EA, Souza RL. Amplification and deletion of the ACHE and BCHE cholinesterase genes in sporadic breast cancer. Cancer Genet Cytogenet. 2010; 197(2):158-65.

45. Willis S, Villalobos VM, Gevaert O, Abramovitz M, Williams C, Sikic BI, et al. Single Gene Prognostic Biomarkers in Ovarian Cancer: A Meta-Analysis. PloS one, 2016; 11(2):e0149183.

46. Zengin T, Önal-Süzek T. Analysis of genomic and transcriptomic variations as prognostic signature for lung adenocarcinoma. BMC bioinformatics, 2020; 21(Suppl 14): 368.

47. Castillo-González AC, Nieto-Cerón S, Pelegrín-Hernández JP, Montenegro MF, Noguera JA, López-Moreno MF, et al. Dysregulated cholinergic network as a novel biomarker of poor prognostic in patients with head and neck squamous cell carcinoma. BMC cancer, 2015; 15: 385.

48. Yoshihara K, Shahmoradgoli M, Martínez E, Vegesna R, Kim H, Torres-Garcia W, et al. Inferring tumour purity and stromal and immune cell admixture from expression data. Nat commun. 2013; 4: 2612.

49. Newman AM, Liu CL, Green MR, Gentles AJ, Feng W, Xu Y, et al. obust enumeration of cell subsets from tissue expression profiles. Nat methods. 2015; 12(5): 453-7.

50. Bindea G, Mlecnik B, Tosolini M, Kirilovsky A, Waldner M, Obenauf AC, et al. Spatiotemporal dynamics of intratumoral immune cells reveal the immune landscape in human cancer. Immunity. 2013; 39(4): 782-95.

51. Olingy CE, Dinh HQ, Hedrick CC. Monocyte heterogeneity and functions in cancer. J leukoc boil. 2019; 106(2):309-22.

52. Sammarco G, Varricchi G, Ferraro V, Ammendola M, De Fazio M, Altomare DF, et al. (2019). Mast Cells, Angiogenesis and Lymphangiogenesis in Human Gastric Cancer. Int J mo sci. 2019; 20(9): 2106.

53. Ma YY, He XJ, Wang HJ, Xia YJ, Wang SL, Ye ZY, et al. Interaction of coagulation factors and tumor-associated macrophages mediates migration and invasion of gastric cancer. Cancer sci. 2011; 102(2): 336-42.

54. Yan Y, Wang LF, Wang RF. Role of cancer-associated fibroblasts in invasion and metastasis of gastric cancer. World J gastroenterol. 2015; 21(33): 9717-26.

55. Chen X, Song E. Turning foes to friends: targeting cancer-associated fibroblasts. Nat rev Drug discov. 2019; 18(2): 99-115.

56. Mao X, Xu J, Wang W, Liang C, Hua J, Liu J, et al. Crosstalk between cancer-associated fibroblasts and immune cells in the tumor microenvironment: new findings and future perspectives. Mol cancer. 2021; 20(1):131.

57. Li L, Wei JR, Dong J, Lin QG, Tang H, Jia YX, et al. Laminin γ2-mediating T cell exclusion attenuates response to anti-PD-1 therapy. Sci Adv. 2021; (6): eabc8346.

58. Li C, Teixeira AF, Zhu HJ, Ten Dijke P. Cancer associated-fibroblast-derived exosomes in cancer progression. Mol cancer. 2021; 20(1): 154.

59. Hu H, Piotrowska Z, Hare PJ, Chen H, Mulvey HE, Mayfield A, et al. Three subtypes of lung cancer fibroblasts define distinct therapeutic paradigms. Cancer cell. 2021; 39(11): 1531-47.e10.

60. Allderdice PW, Gardner HA, Galutira D, Lockridge O, LaDu BN, McAlpine PJ. The cloned butyrylcholinesterase (BCHE) gene maps to a single chromosome site, 3q26. Genomics. 1991; 11(2): 452-4.

61. Vidal CJ. Expression of cholinesterases in brain and non-brain tumours. Chemico-biological interactions. 2005; 157-158: 227-32.

62. Small DH, Michaelson S, Sberna G. Non-classical actions of cholinesterases: role in cellular differentiation, tumorigenesis and Alzheimer's disease. Neurochemistry international, 1996; 28: 453-83.

63. Shan L. (2004). 1-(11)C-Methyl-4-piperidinyl n-butyrate. Molecular

Imaging and Contrast Agent Database (MICAD). Bethesda (MD): National Center for Biotechnology Information (US).

64. Shan L. (2004). Near-infrared dye IRDye 800CW-labeled butyrylcholinesterase. Molecular Imaging and Contrast Agent Database (MICAD). Bethesda (MD): National Center for Biotechnology Information (US).
65. Li B, Duysen EG, Saunders TL, Lockridge O. Production of the butyrylcholinesterase knockout mouse. Journal of molecular neuroscience : MN, 2006; 30: 193-5.
66. Ghebremedhin E, Thal DR, Schultz C, Braak H, Deller T. Homozygosity for the K variant of BCHE gene increases the risk for development of neurofibrillary pathology but not amyloid deposits at young ages. Acta neuropathologica, 2007; 11: 359-63.
67. Scacchi R, Ruggeri M, Corbo RM. Variation of the butyrylcholinesterase (BChE) and acetylcholinesterase (AChE) genes in coronary artery disease. Clinica chimica acta; international journal of clinical chemistry, 2011; 412: 1341-4.
68. Yu R, Guo Y, Dan Y, Tan W, Mao Q, Deng G. A novel mutation in the BCHE gene and phenotype identified in a child with low butyrylcholinesterase activity: a case report. BMC medical genetics, 2018; 19: 58.